Received: 21 May 2025 | Accepted: 16 February 2026

DOI: 10.1111/1365-2745.70289

BRITISH ECOLOGICAL SOCIETY Journal of Ecology

RESEARCH ARTICLE

Enhanced below-ground functioning is associated with higher plant resistance against drought: Implications for ecosystem functions

Alberto Canarini[1,2,3] | Pierre Mariotte[4] | Yolima Carrillo[5] | Raúl Ochoa-Hueso[6] | Jeremy Bougoure[7] | Sotirios Vasileiadis[8] | Ian C. Anderson[5] | Feike A. Dijkstra[9] | Andreas Richter[2] | Hirokazu Toju[3,10,11] | Erica Donner[12,13] | Sally A. Power[5] | Barbara Drigo[5,13,14]

[1]Department of Biological, Geological, and Environmental Sciences (BiGeA), University of Bologna, Bologna, Italy; [2]Centre for Microbiology and Environmental Systems Science, University of Vienna, Vienna, Austria; [3]Center for Ecological Research, Kyoto University, Otsu, Japan; [4]Agroscope, Grazing Systems, Posieux, Switzerland; [5]Hawkesbury Institute for the Environment, Western Sydney University, Penrith, New South Wales, Australia; [6]Department of Biology, IVAGRO, University of Cádiz, Campus de Excelencia Internacional Agroalimentario (CeiA3), Cádiz, Spain; [7]Pacific Northwest National Laboratory, Richland, Washington, USA; [8]Department of Biochemistry and Biotechnology, University of Thessaly, Larissa, Greece; [9]Sydney Institute of Agriculture, School of Life and Environmental Sciences, University of Sydney, Sydney, New South Wales, Australia; [10]Laboratory of Ecosystems and Coevolution, Graduate School of Biostudies, Kyoto University, Kyoto, Japan; [11]Center for Living Systems Information Science (CeLiSIS), Graduate School of Biostudies, Kyoto University, Kyoto, Japan; [12]Future Industries Institute, Adelaide University, Mawson Lakes, South Australia, Australia; [13]Cooperative Research Centre for Solving Antimicrobial Resistance in Agribusiness, Food, and Environments (CRC SAAFE), Mawson Lakes, South Australia, Australia and [14]College of Science, School of Agriculture, Food and Wine, Adelaide University, Urrbrae, South Australia, Australia

Correspondence
Alberto Canarini
Email: alberto.canarini2@unibo.it

Barbara Drigo
Email: barbara.drigo@unisa.edu.au

Funding information
Hawkesbury Institute for the Environment, Western Sydney University; Australian Research Council, Grant/Award Number: FT100100779 and FT130101003; Japan Society for the Promotion of Science; Grant/Award Number: SA PRIF IRGP 45; Future Industries Institute, University of South Australia, Grant/Award Number: PG103515; HORIZON EUROPE European Research Council, Grant/Award Number: 101115960

Handling Editor: Cameron Wagg

Abstract

1. Recent evidence highlights the importance of low-abundant subordinate plant species in regulating ecosystem functions in grasslands experiencing drought via plant–microbe interactions. We hypothesized that subordinate and dominant species have distinct carbon (C) allocation and nitrogen (N) uptake patterns affecting soil microbes and their functions during a drought event.
2. We collected soil cores with individuals of *Paspalum dilatatum* (dominant) or *Cynodon dactylon* (subordinate) from two independent field drought experiments in mesic Australian grasslands. Cores were subjected to a dual-pulse labelling with $^{13}CO_2$ and $^{15}NH_4{}^{15}NO_3$. Stable isotopes were traced in plant biomass and the microbial community (PLFA-SIP, DNA/RNA-SIP and NanoSIM), and soil nutrient cycling was measured via enzymatic activities.
3. The subordinate species invested more C below-ground and had higher N uptake in response to drought compared to the dominant, and the active soil microbial community displayed small but consistent differences. The subordinate species showed higher arbuscular mycorrhizae colonization rates but with similar C exchange to the dominant species in response to drought.
4. *Synthesis*. Our results suggest that the subordinate species achieves higher drought resistance in biomass and soil functions via increased below-ground functioning.

The data presented here provide a basis to explain the underlying mechanisms behind the response of grassland communities and their C cycling to drought.

KEYWORDS
carbon and nitrogen dynamics, dominant plants, drought, ecosystem functioning, microbiome, rhizosphere, subordinate plants

1 | INTRODUCTION

Water is a major determinant of ecosystem functioning. Alterations in water availability such as those derived from extended dry periods (i.e. drought), structures plant and soil microbial communities as well as their interactions (Pugnaire et al., 2019; Van Dyke et al., 2022). However, we lack understanding on how above-ground plant traits link to soil microbial communities and the functions they perform in response to drought. An increasing number of studies have shown that subordinate plant species, defined as those that are found frequently in a community but never attain dominance (Mariotte, 2014), may have a larger influence on ecosystem functioning than their abundance indicates, especially during drought conditions (Boeken & Shachak, 2006; Jia et al., 2021; Mariotte, 2014; Mariotte, Vandenberghe, Meugnier, et al., 2013; Urcelay & Díaz, 2003). Dominant and subordinate species generally have different functional traits, associated with rapid acquisition of resources and with resource conservation, respectively (Diaz et al., 2004; Grime et al., 1997; Mariotte, Vandenberghe, Meugnier, et al., 2013). Above-ground, dominants favour biomass production and subordinates favour nutrient retention (Lavorel et al., 2011), while below-ground, traits of dominant plant species generally promote bacterial-dominated microbial communities, in contrast to the fungal-dominated communities associated with subordinate plant species (de Vries et al., 2012; Grigulis et al., 2013). Given the current increase in drought frequency and intensity in many areas of the world (IPCC, 2023), assessing mechanisms linking the relative abundance of a species and its contribution to ecosystem functioning in response to drought may enhance our ability to predict ecosystem responses to climate change.

Historically, dominant species have been considered more important for ecosystem processes because of the large amount of biomass they produce ('mass ratio hypothesis'; Grime, 1998). However, the biomass of subordinate species often shows higher resistance to drought compared to dominant species (Castillioni et al., 2020; Mariotte, 2014; Mariotte et al., 2015, 2017; Mojzes et al., 2018). It has been suggested that, similarly to keystone taxa in microbial communities (Banerjee et al., 2018), subordinate species may stabilize ecosystem functions within the plant community ('subordinate insurance hypothesis'; Mariotte, 2014) through plant–microbe interactions. Given the importance of plant–soil microbe interactions for multiple ecosystem processes (Van Der Heijden et al., 2008; Wagg et al., 2014), responses to drought at the root-soil interface may have large effects on ecosystem functions. Experimental evidence in a montane grassland in Switzerland has shown that the presence of subordinate species maintains higher ecosystem respiration rates during drought periods and this effect was largely due to the stimulation of soil fungi (Mariotte et al., 2015; Mariotte, Vandenberghe, Kardol, et al., 2013). Given the important role of soil microbial communities in decomposition of soil organic matter (SOM), the effects of plants on soil microbial communities can have important consequences for global carbon (C) and nutrient cycles in response to climate change (Conant et al., 2011; Hursh et al., 2017; Qin et al., 2019).

The response of dominant versus subordinate species to drought may differ because the colonization by arbuscular mycorrhizal fungi (AMF) can increase in subordinate species under drought and they possess a higher C to nitrogen (N) stoichiometric flexibility (Mariotte et al., 2017). In contrast, traits of dominant species (such as nutrient homeostasis and large biomass formation) that allow them to attain dominance (Yu et al., 2015) may be less advantageous when nutrients and water become limited (Mariotte et al., 2017). Therefore, subordinate species may be able to utilize niches created by the decreased competition between dominant and subordinate species during drought, possibly via investing relatively more C into arbuscular mycorrhizal cooperation to obtain soil nutrients such as N. Supporting this, a previous field drought experiment has shown that mycorrhizal arbuscule root colonization correlated positively with plant N in the subordinate species *Cynodon dactylon*, while no correlation was found in the dominant species *Paspalum dilatatum* (Mariotte et al., 2017). Furthermore, arbuscular mycorrhizal symbiosis can reduce the competition between subordinate and dominant plant species (Mariotte, Meugnier, Johnson, et al., 2013), although the direction of this effect depends on the type of mycorrhizal fungi and environmental conditions (Lin et al., 2015; Yao et al., 2008). The accumulated evidence suggests that mycorrhizal fungi represent an important regulator of plant–plant interactions, minimizing fitness differences between plant species and regulating plant community dynamics (Bever et al., 2010; Urcelay & Díaz, 2003) and are linked to ecosystem processes such as nutrient cycling and plant productivity (Wipf et al., 2019). However, we have limited experimental evidence linking mycorrhizal colonization, soil nutrient cycling and the dynamics of dominant versus subordinate plant species under drought, despite the potential in shaping the composition and biomass of grassland communities. Given that grasslands are one of the most widespread biomes, accounting for up to 40% of the emerged land surface (Petermann & Buzhdygan, 2021), and their role in biodiversity conservation and carbon sequestration, this represents an important knowledge gap.

In this study, we aimed at quantifying below-ground C investment and N uptake traits of a dominant (*Paspalum dilatatum*) and a subordinate (*Cynodon dactylon*) grass species in two Australian grasslands exposed to experimental drought. Specifically, we hypothesized that:

(i) the dominant species allocates more C above-ground per unit of N while the subordinate species allocates more C below-ground, that is to the microbial community;
(ii) the subordinate species increases C allocation to arbuscular mycorrhizae during drought;
(iii) the subordinate species obtains more N during drought conditions.

To assess these hypotheses, we made use of two field drought experiments that had similar plant species composition and climate but different soils. At both sites, dominant species decreased their biomass in response to drought, while subordinate species either increased or did not change their biomass. Intact soil cores with either the dominant *P. dilatatum* or the subordinate *C. dactylon* were collected and subjected to a $^{13}C\text{-}CO_2$ and $^{15}NH_4{}^{15}NO_3$ dual-pulse labelling incubation to measure species-specific C and N trading at the plant–soil interface.

2 | MATERIALS AND METHODS

2.1 | Study systems

The field experiment was carried out in two semi-natural Eastern Australian grasslands: (i) John Bruce Pye Farm (hereafter referred as 'JP'), The University of Sydney, approximately 30 km north-west of Campbelltown, NSW, Australia (33°56′25.5″ S 150°40′15.5″ E) (Canarini, Carrillo, et al., 2016); and (ii) the 'Drought and Root Herbivore Impacts on Grassland' (DRI-Grass) experimental facility (from here now referred as DG), located at the Hawkesbury Institute for the Environment, at Western Sydney University, Richmond, Australia (33°36′35.0″ S 150°44′18.0″ E) (Power et al., 2016). Fieldwork was conducted at research sites managed by the University of Sydney and Western Sydney University. As the research was carried out by authorized researchers within institutionally managed sites, no additional fieldwork permits or licences were required. The two experiments were 37 km apart and experienced similar climatic conditions. The climate of the area is temperate with hot wet summers (December to February) and cool dry winters (June to August). The experimental design of the two experiments is described in detail in Canarini, Carrillo, et al. (2016) and Power et al. (2016), respectively. A summary of each site's climate, soil properties and a list of the dominant and subordinate species are given in Table S1. In this study, we used a sub-set of 8 sheltered plots from each experiment representing two simulated rainfall regimes with four replicates each: (i) ambient rainfall (hereafter 'Control') and (ii) reduced rainfall quantity by 50% (hereafter, 'Drought'). Drought was applied as a continuous 50% reduction in ambient rainfall throughout the year for the full duration of the experiment. The above-ground biomass of subordinate species increased at the DG site and remained constant at the JP site under drought whereas dominant species decreased their biomass at both sites (Figure S1; see also Mariotte et al., 2017).

2.2 | Soil core sampling and growth chamber incubation

In the summer of 2016, after about 2 years of reduced rainfall manipulation at the JP site and 2.5 years at the DG site, two 10 cm diameter areas within each plot in each site were selected to contain one of the two species of interest: the subordinate *Cynodon dactylon* or the dominant *Paspalum dilatatum*. The experimental drought (as well as the controls) was still ongoing at the time of core collection. These species were chosen because they were classified as dominant/subordinate at both sites based on their frequency and cumulative relative cover (Mariotte, 2014; Mariotte et al., 2017) and were present in all plots. Ten cm diameter × 20 cm deep PVC sections were inserted into the ground down to 15 cm and the resulting cores removed, transported to the laboratory and placed in a growth chamber. Due to the clonal and tufted growth form of both grass species, it was not possible to confirm whether each core contained a single genet or multiple interconnected individuals. However, all cores were visually inspected and confirmed to be monospecific, with only the target species (*Cynodon dactylon* or *Paspalum dilatatum*) present. Cores were incubated in two controlled CO_2 (one for ^{13}C labelling and one for natural abundance) flow cabinets (2 m × 2.4 m × 1 m; Climatic Chambers, Vancouver, Canada). Cores were physically separated in trays and labelling was performed in isolated CO_2 flow cabinets to prevent cross-contamination. Each cabinet provided an airtight system (1500 L airtight units) enabling the maintenance of a constant atmospheric CO_2 level of 400 μL L^{-1}. The CO_2 concentrations were maintained automatically using mass flow controllers (Brooks Smart, DMFC, Emmerson process Management, Pittsburg, PA, USA). A broad infrared gas analyser (IRGA, CARBOCAP, GMT222, Dual Wavelength NDIR sensor, Vaisala, Oyj, Finland) was fitted in each of the flow cabinets to control the correct delivery of CO_2. The concentrations of CO_2 were maintained at 400 μL L^{-1} by a solid carbon soda filter (Sofnoline, Sigma, St Louis, MO, USA). In each cabinet, maximum daily temperatures ranged from 25 to 26°C; daily minimum temperatures ranged from 15 to 16°C. Light intensity averaged 250 W m^{-2}, with a 16-h photoperiod and a relative humidity of 70%. Climate data for the cabinet were stored digitally during the entire incubation period. Cores from drought field plots were maintained at 10% gravimetric water content and those from control plots at 20%. These target gravimetric water values were based on typical field conditions at the field sites in the 2014–2016 summers (Canarini, Carrillo, et al., 2016; Ochoa-Hueso et al., 2020). Once the target moisture level was reached, it was maintained with daily watering. All cores were randomly redistributed after each watering period to reduce potential position effects within the growth chamber. A schematic illustration summarizing the experimental design and analyses is provided in Figure 1.

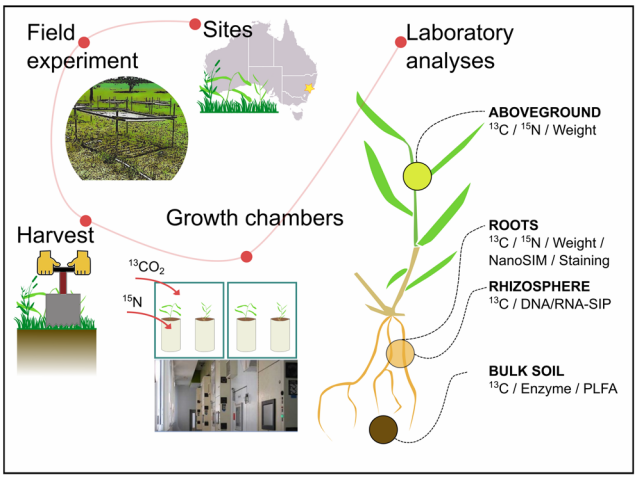

FIGURE 1 Schematic illustration of the experimental design and laboratory analyses.

2.3 | $^{13}CO_2$ and ^{15}N dual-pulse labelling

After 10 days under simulated Control and Drought conditions, each core received 50 mL of water containing 35 mg of 98 atom % $^{15}NH_4{}^{15}NO_3$ (equalling 45 kg N ha^{-1} per each 10 cm pot), which was applied by pouring slowly from above avoiding contact with the plant. We applied $^{15}NH_4{}^{15}NO_3$ to the soil surface to label the mineral N pool accessible to roots and arbuscular mycorrhizal fungi within intact cores. Plants were returned to the chamber for 1 day to allow for water and N uptake. After that, $^{13}CO_2$ pulse-labelling (99 atom % ^{13}C-CO_2, <3 atom % ^{18}O; Sigma-Aldrich, Germany) was carried out at 400 μL L^{-1} for 24 h. A total of 32 soil cores were used in the pulse-labelling experiment. Fourteen cores of *C. dactylon* (7 under drought condition and 7 controls) and 14 cores of *P. dilatatum* (7 under drought condition and 7 controls) with equal representation from the two field sites were labelled with $^{15}NH_4{}^{15}NO_3$ and subjected to the $^{13}CO_2$ pulse labelling. An additional 4 unlabelled cores (2 per species) served for natural abundance and background ^{15}N and ^{13}C measurements and were incubated in a separate CO_2 flow cabinet to ensure that there was no contamination with respired ^{13}C-enriched CO_2. Isotopic enrichment (excess ^{13}C and ^{15}N) was calculated as the difference between labelled and natural abundance samples using a mass balance approach. For each pool, the atom% excess was multiplied by the total mass of C or N, following the approach of Drigo et al. (2010), but adapted here to integrate both plant and microbial compartments. The ^{13}C and ^{15}N 'excess' in each pool was calculated as a simple mass balance relative to unlabelled controls:

$$\text{Excess}^{13}C_{pool} = C_{pool} \times \left(\text{atom}\,\%\,{}^{13}C_{labeled} - \text{atom}\,\%\,{}^{13}C_{natural}\right) / 100$$

$$\text{Excess}^{15}N_{pool} = N_{pool} \times \left(\text{atom}\,\%\,{}^{15}N_{labeled} - \text{atom}\,\%\,{}^{15}N_{natural}\right) / 100$$

where C_{pool} and N_{pool} are the total C or N masses of the pool (shoots, roots, rhizosphere soil, bulk soil; units as reported). Whole-core recovery was computed as the sum across pools.

2.4 | Harvesting procedure, soil and plant $^{13}C/^{15}N$ analysis and root staining

To assess the fate of ^{13}C and ^{15}N, we sampled all labelled *C. dactylon* and *P. dilatatum* plants and soil immediately after the 24 h of labelling. In addition, four unlabelled *C. dactylon* and *P. dilatatum* were harvested to serve as controls for background δ^{13}C and ^{15}N values. Upon harvest, shoots, roots, rhizosphere soil and bulk soil were separated. Half of the shoot samples were oven-dried and weighed, and the other half freeze-dried for ^{13}C and ^{15}N analysis. Roots were shaken gently to remove loosely adhering soil, and the remaining attached soil was considered rhizosphere soil. Root fragments remaining in the bulk or rhizosphere soil samples were removed by passing through a 1 mm sieve. A portion of the soil samples (rhizosphere for RNA-stable isotope probing [SIP] and bulk for PLFA) were frozen immediately in liquid N, freeze-dried (bulk soil only) and stored at −80°C until analysis. Clean root samples were high-pressure frozen (Leica Microsystems, Australia) and stored at −80°C before further sample preparation for ^{13}C and ^{15}N by high resolution mass spectrometry (NanoSIMS).

All plant parts and soils were analysed for total C and N content and $^{13}C/^{15}N$ abundance by a Delta V Advantage isotope ratio mass spectrometer (IRMS) with a Conflo IV interface (Thermo Fisher Scientific, Bremen, Germany). A portion of the collected roots was cleared in 10% KOH while fresh and stained with an ink-vinegar solution containing 5% Parker Quink Blue in household vinegar (adapted from Vierheilig et al., 1998). For each subsample, three fine roots (<1 mm) of approximately 2.5 cm in length were examined under the microscope (Leica DM 2500M, Leica Microsystems, Wetzlar, Germany) for the presence of mycorrhizae using the modified line intersection method (McGonigle et al., 1990). Presence of hyphae, arbuscules or vesicles was recorded on 50 intersections for each of three roots (total of 150 intersections per sample) and used to estimate the percentage of root colonization, which was then averaged. Subsamples of fresh bulk soil were used for enzymatic activity measurements as detailed below.

2.5 | DNA and RNA SIP

Total RNA was extracted from 300 mg rhizosphere soil samples using the RNeasy PowerSoil Total RNA kit (QIAGEN, Australia) according to the manufacturer's instructions. From the same lysates, genomic DNA was purified using the RNeasy PowerSoil DNA Elution Kit (QIAGEN), following the manufacturer's instructions, yielding matched RNA and DNA from each sample. The integrity of the RNA preparations was visualized by LabChip® microfluidic technology and automated electrophoresis for RNA analysis using the Experion RNA StdSens analysis system (ExperionTM, Bio-Rad Laboratories Inc., Australia). Total RNA was quantified using both the ExperionTM system and a NanoDrop, ND-1000 4 Spectrophotometer (Bio-Rad Laboratories Inc., Australia) and subsequently stored at −80°C. ^{13}C and ^{15}N enriched Extracted RNA/DNA was separated by isopycnic centrifugation in CsTFA gradients (60 h, 45,000 rpm). Fractions were collected, and 'heavy'

DNA and RNA were identified by buoyant density and confirmed via RT-qPCR amplification (Drigo et al., 2010). RNA samples from equilibrium density gradient fractions were reverse transcribed using Moloney Murine Leukaemia Virus reverse transcriptase with low RNAse H activity (200 U μL^{-1}, M-MLV Reverse Transcriptase, Thermo Fisher Scientific, Australia) using random hexamer primers (0.2 $\mu g\,\mu L^{-1}$), according to the manufacturer's protocol. The resulting cDNA was then used for bacterial 16S rRNA and fungal 18S rRNA quantification by real-time PCR (see Supporting Information: Materials and methods for more details). The diversity analysis was performed by sequencing the polymerase chain reaction (PCR) amplified V4 bacterial 16S rRNA gene hypervariable (V) region for bacteria, the intergenic spacer (ITS2) between the 5.8S rRNA gene and the large ribosomal subunit (28S rRNA) coding gene for fungi. ITS2 amplification was performed from extracted DNA and analysed separately from RNA-derived data. The PCR products were prepared in two reactions. A low-cycle (28 cycles) reaction for amplifying the target sequences using primers suitable for the target microbial groups and one (8 cycles) for indexing the amplified sequences with the same primers containing the indexing and linker 5′ overhangs ('Primers_indexes.xls' file) generated with the Barcrawl v100310 software (Frank, 2009). The selected two-step strategy aimed to prevent index-associated biases during amplification in cases where indexed primers are used directly on environmental DNA templates (Berry et al., 2011). For more details regarding primer sets, products quantification and cycling conditions and for the bioinformatic pipeline see Supporting Information: Materials and methods.

2.6 | PLFA and NLFA analysis

Soil phospholipid and neutral lipid fatty acid (PLFAs and NLFAs, respectively) were extracted from bulk soil samples and analysed using the high throughput method described in Buyer and Sasser (2012) and adapted for collecting NLFAs (Sharma & Buyer, 2015). Briefly, 2 g of freeze-dried bulk soil was used for Bligh–Dyer lipid extraction (Bligh & Dyer, 1959) as detailed in Castañeda-Gómez et al. (2020). All samples were dried and analysed with gas chromatography (GC; Trace 1300, Thermo Scientific, Austria) coupled to an ISQ single quadrupole mass spectrometer (MS; Thermo Scientific, Germany) following *trans*-esterification for quantitative analysis relative to an internal standard (19:0). PLFA-specific $\delta^{13}C$ values were analysed using a Trace GC Ultra connected by a GC-IsoLink to a Delta V Advantage Mass Spectrometer (all Thermo Fisher Scientific) with the same program as the GC–MS. We used branched PLFAs (i15:0, a15:0, i16:0, i17:0, a17:0, a19:0, a18:0) as indicators for gram-positive bacteria which also includes the 10Me-PLFAs (10Me16:0, 10Me17:0, 10Me18:0) indicators for actinomycetes. We used cyclopropyl and mono-unsaturated PLFAs (16:1ω7, cy17:0 and cy19:0) for gram-negative bacteria, the mono-unsaturated PLFA 16:1ω5 for arbuscular mycorrhizal fungi, saturated PLFA 15:0 for uncategorized bacteria, mono and poly-unsaturated PLFAs (cis18:1ω9 and 18:2ω6,9) for fungi and unspecific PLFAs (16:1, 17:1, 18:1, i19:0, a19:0, trans18:2ω6,9) for viable biomass (Hu et al., 2018). The NLFA 16:1ω5 was also used for arbuscular mycorrhizal fungi, as the PLFA 16:1ω5 can be also found in bacteria (Frostegård et al., 2011). The relative abundance of each PLFA (% of total PLFA C) was used to compare microbial community composition among treatments. The excess ^{13}C recovered in each PLFA was determined by multiplying the mass of PLFA C (μg C g dry $soil^{-1}$) and its atom % excess ^{13}C (measured atom% ^{13}C minus natural abundance atom% ^{13}C). Natural abundance of ^{13}C in each PLFA was determined from unlabelled samples.

2.7 | High resolution imaging mass spectrometry

High-pressure frozen (HPF) root tissue sections were slowly freeze-substituted, resin-embedded and sectioned to 350 nm thickness. Sections were mounted on flat Si wafers and gold coated (10 nm) before analysis on nanoSIMS 50L at the University of Western Australia (Bougoure et al., 2014). The NanoSIMS-50L analysis was done with a 16 keV Cs^+primary ion beam in multi-collection mode and trolleys positioned to simultaneously detect the negative secondary ions ^{16}O, ^{18}O, $^{12}C_2$, ^{13}C, ^{12}C, ^{14}N, ^{15}N and ^{31}P. The mass spectrometer was tuned to high mass resolution of c. 10,000 (CAMECA definition) to separate the $^{12}C^{15}N$ from the $^{13}C^{14}N$ peak on mass 27 allowing determination of $^{15}N/^{14}N$, $^{13}C/^{12}C$ ratios and $^{18}O/^{16}O$ ratios as well as ^{31}P and secondary electron imaging (for identification of cellular and sub-cellular structures). Prior to analysis, selected areas of interest were sputtered (Cs^+implanted) by rastering a defocused primary ion beam (current density 2.5×10^{15}ions cm^{-2}) over a slightly larger area to allow samples to reach sputtering equilibrium (60 ms $pixel^{-1}$). Generally, analysis was performed in a chained method to allow 'stitching together' of many smaller images (30 μm^2; 256 × 256 pixels) to create a single larger image (e.g. Figure S5) of entire root cross sections. This approach is useful for minimizing sample spot bias and analysing co-occurring organisms.

A correction factor was applied to all NanoSIMS data to make it directly comparable to isotope ratio mass spectrometry (IRMS) data. The correction factor was based on analysis of a yeast (*Saccharomyces cerevisiae*) standard with known $^{15}N/^{14}N$ and $^{13}C/^{12}C$ abundance. Images were processed and analysed using the OpenMIMS data analysis software plugin in ImageJ (https://github.com/BWHCNI/OpenMIMS). Single images were stitched together using nrrd mosaics script (available and described at https://github.com/BWHCNI/OpenMIMS/wiki/nrrd-Mosaics). NanoSIMS imaging was used to quantify ^{13}C and ^{15}N enrichment at the cellular level within root cross sections. Isotope maps were interpreted in the context of root anatomical features, including epidermis, cortex and stele, as well as fungal structures such as arbuscules where visible. Enrichment in the stele was interpreted as indicative of plant nitrogen uptake, while localized enrichment in cortical regions with AMF structures suggested sites of nutrient exchange or carbon allocation to symbionts.

2.8 | Enzymatic activity measurements

Hydrolytic extracellular enzyme activities are a good proxy of the potential of soil microbial communities to process soil organic matter and thus of their functioning in soils (Sinsabaugh et al., 2008). These enzymes can be related to the processing of organic molecules rich in different key elements such as C, N, phosphorus (P) and sulphur (S). Enzymes assayed in our study were: α-1,4-glucosidase (AG; starch degradation), β-1,4-glucosidase (BG; starch degradation), β-xylosidase (XYL; hemicellulose degradation) and β-D-cellobiohydrolase (CBH; cellulose degradation) for the C cycle; β-1,4-N-acetylglucosaminidase (NAG; chitin degradation) and L-leucine aminopeptidase (LAP; protein degradation) for the N cycle; acid phosphatase (PHOS; P mineralization) for the P cycle; and aryl-sulfatase (AS; S mineralization) for the S cycle. Soil enzyme activities were assessed fluorometrically following the methods described in Bell et al. (2013). Briefly, assays were conducted by homogenizing 0.3 g of rhizosphere soil for both *P. dilatatum* and *C. dactylon* in 30 mL of 50 mM sodium acetate buffer (pH 6.5) for 1 min. The homogenized solutions were then added to a 96-deep-well (2 mL) microplate. Control replicates of soil slurry and 4-methylumbellfferone (MUB) or 7-amino-4-methylcoumarin (MUC) standard curves of 0–100 μM were included in each sample. Soil slurries with fluorometric substrates (Sigma-Aldrich: M9766 for AG, M3633 for BG, M7008 for XYL, M6018 for CBH, M2133 for NAG, L2145 for LAP, M8883 for PHOS and M7133 for AS) were then incubated for 1.5 h at 35°C. Following incubation, the supernatant solution was transferred into corresponding wells in a black, flat-bottomed 96-well plate. The plates were then scanned on a microplate fluorometer (2300, EnSpire® Multilabel Reader, PerkinElmer, Boston, MA, USA) using an excitation wavelength of 365 nm and an emission wavelength of 450 nm.

We analysed the nutrient acquisition strategies of the entire community by calculating the stoichiometric ratio of enzymes. The C:N:P:S acquisition ratio is a key characteristic that describes the functions of the soil microbial community, connecting environmental nutrient availability to the C:N:P:S stoichiometry of microbial biomass (Sinsabaugh et al., 2008; Waring et al., 2014). We calculated stoichiometric ratios of microbial acquisition strategies by dividing the natural logarithm of enzymatic activities related to the C-cycle (BG, AG, XYL, CBH) by either N cycle-related enzymes (NAG, LAP) or P cycle-related enzyme (PHOS) or S cycle (AS) (Sinsabaugh et al., 2008; Waring et al., 2014).

2.9 | Statistical analyses

All statistical analyses were carried out with R version 3.6.3 (R Core Team, 2020). All single variables were analysed with a linear mixed effect model using the *lme* function of the 'nlme' package (Pinheiro et al., 2017). Each species × treatment combination included cores from both JP and DG sites (minimum $n = 3$ per site). Site, treatment (Control vs. Drought) and plant group (dominant vs. subordinate) were used as fixed factors to assess individual and interactive effects. Plot number was used as a random factor. We checked for homogeneity of variances and normality of residuals by inspecting the plot of standardized residuals versus predicted values, frequency histogram and QQ-plot (Kozak & Piepho, 2018). When normality of residuals and/or homogeneity of variance was not met, variables were log-transformed. *P*-values of the chosen model were generated using the function *anova*, and the significance threshold was set to 0.05. Multivariate statistical analysis for PLFA and enzyme data was carried out using the function *adonis* of the R package 'vegan' (Oksanen et al., 2013) to assess individual and interactive effects of site, treatment and plant group. Permutations were set at 999. Data were transformed into relative abundance for PLFA and ^{13}C-enrichment in PLFA, whereas to account for the different methods of measuring enzyme activities, data were scaled to unit variance with the function '*scale*'.

Following amplicon sequencing, data handling and manipulation were undertaken using the phyloseq package (McMurdie & Holmes, 2013). Data were filtered by removing sequences matching '*Mitochondria*', '*Chloroplast*' and '*Eukaryota*' from the archaeal and bacterial community, and by removing '*Protista*' and unknown domains from the fungal community. In order to minimize the inflation of rare ASVs in the community analysis, we removed ASVs that had less than 10 reads in at least 2 samples per treatment (Straub et al., 2020). Rarefaction curves were generated for all filtered samples. Appropriate subsample depth was established by visual inspection of rarefaction curves to ensure adequate sample depth (Figure S2). Some samples were excluded from the analysis due to low sequencing depth (16S data set = 6 samples excluded; ITS data set = 8 samples excluded; Figure S2). This left 3799 ASVs in the 16S dataset and 2615 ASVs in the ITS data set. The filtered ASV matrix was used for all downstream analyses concerning amplicon sequencing data. Data normalization for β-diversity analysis was carried out using the centred log-ratio transformation. Multivariate statistical analysis was carried out as described above for PLFA. Dataset streamlining was performed with the R package 'Prevalence Interval for Microbiome Evaluation' (pime) v0.1.0 (Roesch et al., 2020) that was used for selecting ASVs of optimal prevalence among treatment levels for obtaining the lowest possible random forest out of bag (OOB) error rates. An optimal prevalence cut-off was selected as the percentage that retained at least 1/5 of the initial sequences and returned the lowest possible OOB error in the random forest run with the retained amplicon sequencing variants (ASVs). Following this, differential abundance testing was performed using the reduced dataset via the implementation of the ANCOM-BC2 v1.4.0 R package main algorithm providing global (ANOVA-like) and pairwise comparisons (*t*-test analogue) (Lin & Peddada, 2024), employing the Holm method for multi-level and multiple hypothesis testing *p*-value adjustment. Plots were generated using the *ggplot2* package (Wickham, 2016).

3 | RESULTS

3.1 | Subordinate species increase C allocation below-ground and N uptake

The chosen plant individual did not present any difference between species, drought or site in above-ground and below-ground biomass, and root to shoot ratio (Figure S3; Table S2). Despite

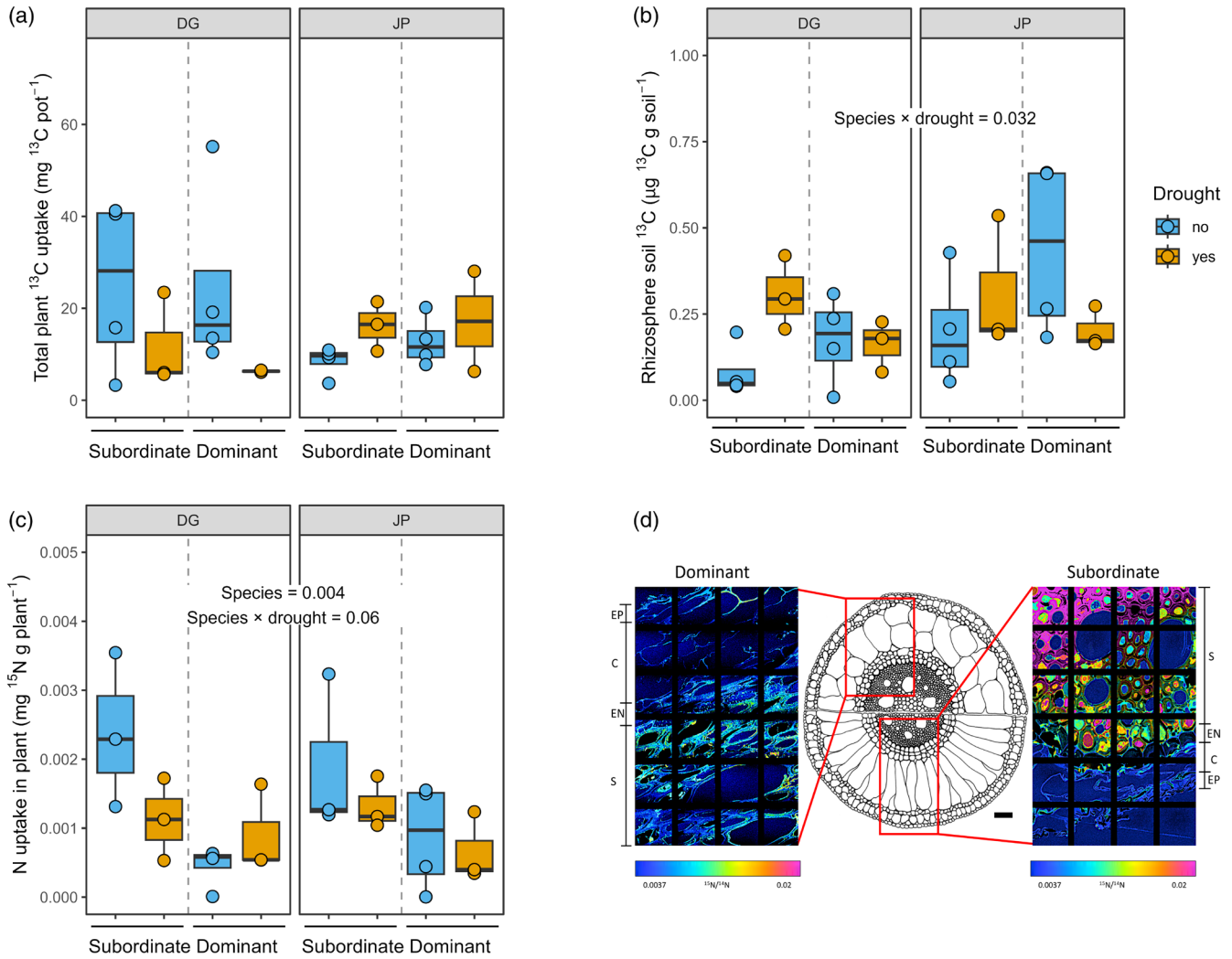

FIGURE 2 Graph showing effects of drought, species and sites on (a) total plant ^{13}C uptake (mg ^{13}C pot^{-1}); (b) ^{13}C accumulation in rhizosphere soil (µg ^{13}C g soil^{-1}); (c) N uptake in plant (mg ^{15}N g plant^{-1}). Significant results are shown on top of the graphs (when $p < 0.05$). Box centre line represents median, box limits the upper and lower quartiles, whiskers the 1.5× interquartile range, while separated points represents outliers. (d) NanoSIMS generated ^{15}N/^{14}N HIS images of ^{15}N accumulation in the dominant (left) and subordinate (right) species. Images are representative root cross sections (central image) for the two species under drought conditions (C, cortex; EN, endodermis; EP, epidermis; S, stele).

similar accumulation of ^{13}C in plant biomass across treatments (Figure 2a; non-significant differences Table S2), we found consistently higher ^{13}C accumulation in the rhizosphere soil of subordinate species (*C. dactylon*) under drought (Figure 2b; species × drought: $p = 0.032$; Table S2). A similar result was found in bulk soil (Figure S2; Table S2) without any increase in root to shoot ratio of measured ^{13}C (Figure S4; Table S2). Furthermore, the subordinate species showed lower values of above-ground C:N ratio (Figure S3; Table S2).

Plant N uptake (^{15}N incorporation) showed a significant effect of species (Figure 2c; $p = 0.004$) and a marginally (p-value between 0.05 and 0.1) significant species × drought interaction ($p = 0.06$). The NanoSIMS data support the IRMS data indicating higher ^{15}N accumulation in the subordinate species with most of the ^{15}N found in the stele (Figure 2d). Transfer of ^{13}C and ^{15}N uptake in arbuscular mycorrhizae was also visualized via NanoSIMS images, although only successfully obtained for the dominant plant species due to insufficient image quality for the subordinate species samples (Figure S5).

3.2 | Both plant species allocate similar amount of C to arbuscular mycorrhizae

Mycorrhizal root colonization was significantly higher for the subordinate species (Figure S6c; species: $p < 0.0001$; Table S3), with arbuscules being more abundant and increasing under drought for this species only (Figure 3a; species × drought: $p = 0.005$; Table S3). The 16:1ω5 biomarker obtained from NLFA and PLFA was used as a signature for AMF biomass and ^{13}C incorporation (Olsson & Lekberg, 2022), where increased ^{13}C in NLFA suggests enhanced production of AMF storage organs or spores, whereas in PLFA, it indicates AMF growth stimulation. We did not find any significant effect of species in either PLFA or

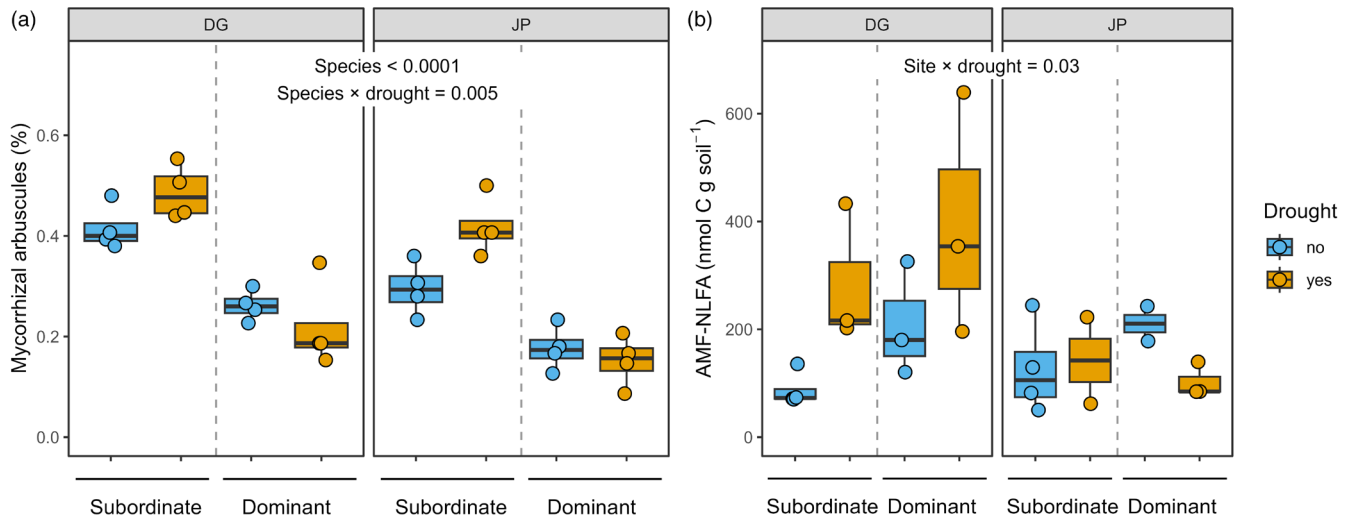

FIGURE 3 Graph showing effects of drought, species and sites on (a) mycorrhizal arbuscules in roots (%) and (b) arbuscular mycorrhiza NLFA biomarker (nmol C g soil^{-1}). Significant results are shown on top of the graphs (when $p < 0.05$). Box centre line represents median, box limits the upper and lower quartiles, whiskers the 1.5× interquartile range, while separated points represents outliers.

NLFA 16:1ω5 biomarker. The NLFA arbuscular mycorrhizal biomarker showed a site by treatment interaction (Figure 3b; $p = 0.032$), and in general, it displayed a higher increase in response to drought in the subordinate species, although not significant. Its PLFA counterpart was positively affected by drought (Figure S6b; Table S3). The amount of ^{13}C present in the AMF biomarkers (PLFA and NLFA) showed no overall significant effects (Figure S6c,d; Table S3).

3.3 | The active microbial community displays small but consistent differences between drought and species

Total amount of PLFA in bulk soil increased with drought (Figure S7a; Table S4), whereas the total amount of ^{13}C in PLFA was not affected by drought, site or species identity (Figure S7b; Table S4). The relative abundance of the main microbial groups defined by PLFA was similar between treatments and sites (Figure 4a). Drought increased most bacterial group absolute abundances (Figure S7; Table S4). The ^{13}C relative distribution was clearly affected by drought (Figure 4b), with most groups decreasing, except for fungi and general biomarkers (Figure S7; Table S4). When individual PLFA biomarkers were used as a fingerprint for community composition, we found an effect of site (Figure 4c; $p < 0.001$; $R^2 = 0.16$; Table S5) and drought ($p < 0.001$; $R^2 = 0.15$) on community composition, indicating that changes in community composition at the PLFA level were not affected by species. The ^{13}C in PLFA biomarkers was used in the same way to indicate community composition of the active (^{13}C consuming microbes) portion of the soil microbial community. We found effects of drought (Figure 4d; $p < 0.001$; $R^2 = 0.37$; Table S5) and species ($p = 0.023$; $R^2 = 0.09$), indicating that these two factors were the main regulator of C partition within the soil microbial community.

The active microbial community analysed by DNA/RNA-SIP (actively metabolizing ^{15}N and ^{13}C) revealed similar composition across treatments (Figure S8; Table S5). Statistical analysis revealed that there were also no overall significant treatment effects on gene copy numbers (qPCR; Figure S9). Differential abundance analysis revealed differences only with the bacteria community. We focused here on the family level, where the global test showed group difference among 7 families (Table S6). Within these families, pairwise tests showed significant results only for members of the *Rhizobiaceae*, which were positively increased in the rhizosphere of the subordinate species during drought conditions compared to control conditions, and in the members of the *Enterobacteriaceae* which were positively increased in the rhizosphere of the subordinate compared to the control of the dominant species (Table S6; Figure S10).

3.4 | Plant species modify acquisition strategies of soil microbial communities

Soil processes measured by eight different enzyme activities mainly differentiated by site, as revealed by PERMANOVA analysis (Figure 5a; $p = 0.014$; $R^2 = 0.14$; Table S7). We analysed the nutrient acquisition strategies of the overall community, calculated as the stoichiometric ratio for enzymes involved in the C, N, P and S cycles. The acquisition ratio is an integral feature to describe soil microbial community functions, linking environmental nutrient availability to the stoichiometry of microbial biomass (Sinsabaugh et al., 2008; Waring et al., 2014). We found that acquisition strategies were mainly affected by drought (which decreased the C to nutrient ratios) and by species (lower C to nutrient ratios in the dominant species; Figure 5b–d; Table S7). We also found a significant site effect for the enzyme C:N ratio ($p = 0.0005$).

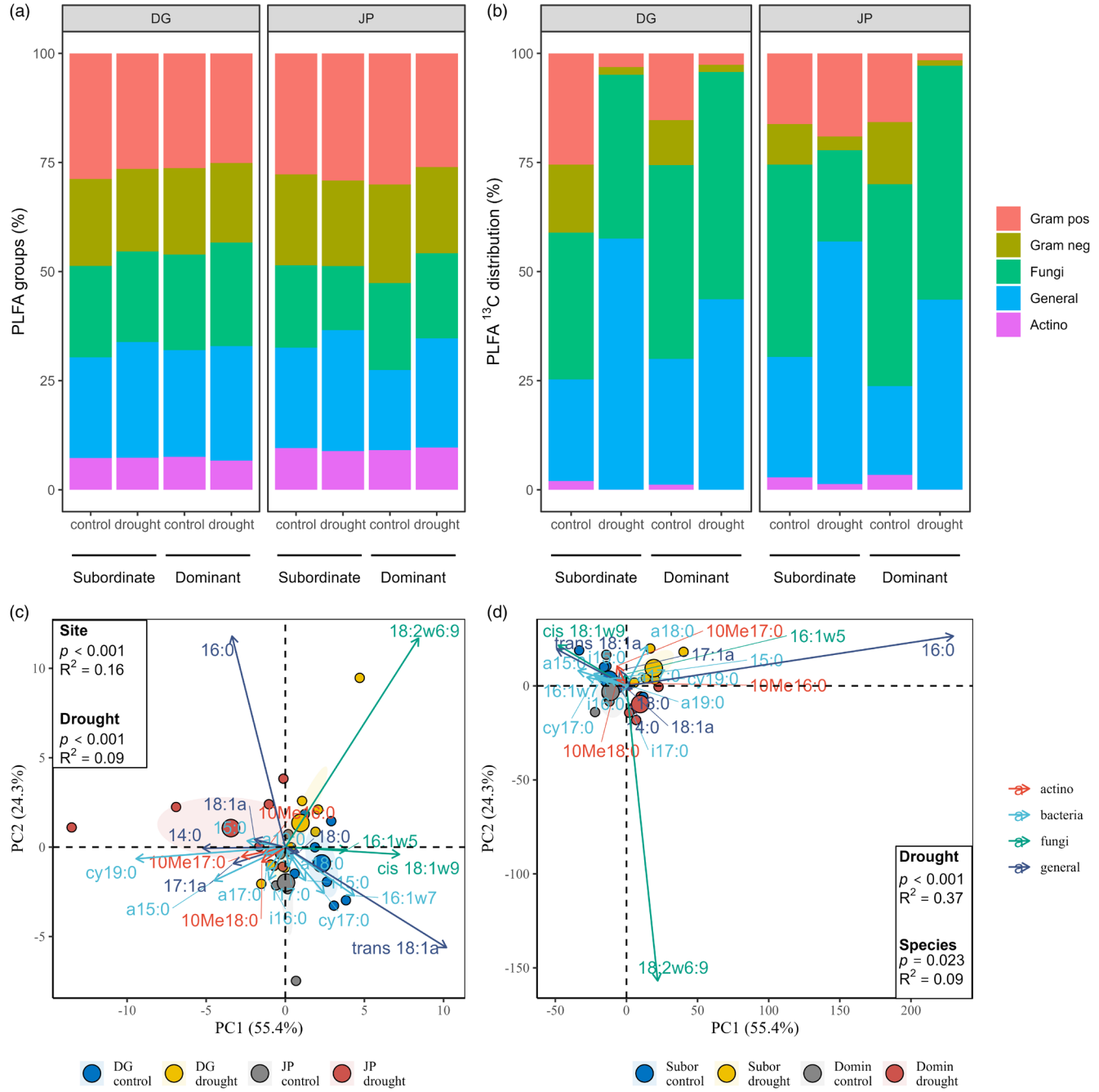

FIGURE 4 Graphs showing effects of drought, species and sites on PLFA biomarkers. Top graphs show the relative distribution of PLFA (a) and ^{13}C in PLFA (b) between main taxonomic groups. Bottom graphs represent the Principal Component Analysis (PCA) plot of the relative distribution of PLFA (c) and ^{13}C in PLFA (d) in the analysed biomarkers. Significant results from the Permanova analysis are shown on top of the graphs (when $p < 0.05$). Values are coloured according to the significant results (c = drought and site; d = drought and species; Subor = Subordinate species; Domin = Dominant species), larger circles represent the centroid for each group and ellipse the 95% confidence interval. PLFA biomarkers are coloured by the taxonomic group.

4 | DISCUSSION

Recent evidence has demonstrated an important role of subordinate plant species in regulating ecosystem functions during drought events, via plant–soil microbe interactions (Mariotte et al., 2015, 2017). Since an increase in the severity and frequency of drought events is predicted in many areas of the world (IPCC, 2023), understanding the mechanisms behind the importance of subordinate species for ecosystem functioning under drought can improve our understanding of climate change effects on ecosystems. Here, we show subordinate-specific features of C allocation, N uptake and interaction with the soil microbial community during drought, which could elucidate broader community dynamics and ecosystem functions in response to drought stress in grasslands, one of the most extensive biomes on Earth.

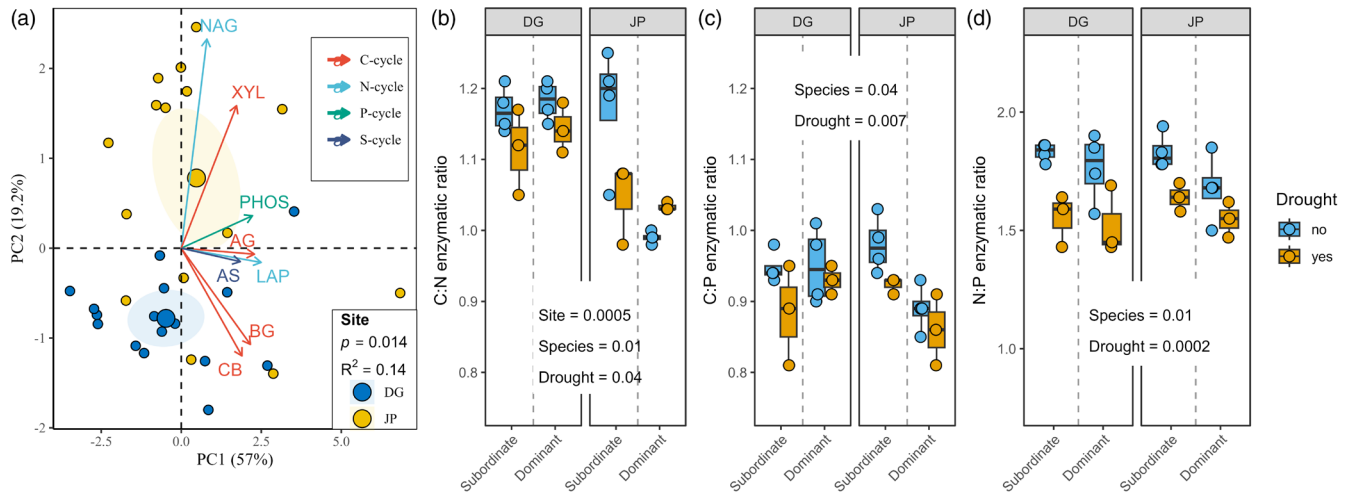

FIGURE 5 Graphs showing effects of drought, species and sites on enzyme activities and acquisition strategies. Left graph (a) represents the PCA plot of the normalized potential enzymatic activities. Significant results from the Permanova analysis are shown on the graph (when $p < 0.05$). Values are coloured by site; larger circles represent the centroid for each group and ellipse the 95% confidence interval. Individual enzymes are coloured by the elemental cycle group. Right graphs represent the acquisition strategies, quantified as stoichiometric ratios of enzymatic activities of C:N (b), C:P (c) and C:S (d). Significant results are shown on top of the graphs (when $p < 0.05$). Box centre line represents median, box limits the upper and lower quartiles, whiskers the 1.5× interquartile range, while separated points represent outliers.

The subordinate species (*C. dactylon*) showed a larger C allocation to soil (rhizodeposition) compared to the dominant species (*P. dilatatum*; Figure 2). While we found no previous studies examining C allocation to soil by subordinate versus dominant species, rhizodeposition exerts an important influence on C and nutrient cycling (Canarini et al., 2019), with grasslands showing a wide spectrum of species-specific root exudate strategies (Williams et al., 2021). Drought can modulate root exudate quality and quantities, with species-specific responses (Canarini, Merchant, & Dijkstra, 2016) and this can alter ecosystem C cycling. de Vries et al. (2019) found higher soil respiration rates from root exudates collected from plants subjected to drought compared to those collected from non-droughted plants. Therefore, it was suggested that root exudates have important consequences for ecosystem functions during drought (Williams & de Vries, 2020) and that accumulation of C during drought facilitates high microbial activity during rewetting events (Karlowsky et al., 2018). In this experiment, ^{13}C respiration was not quantified and therefore the increased ^{13}C in soil might be due to different C utilization by the soil microbial communities under the subordinate and dominant species. However, measurement of total, as well as group-specific, ^{13}C incorporation into microbial biomass did not show significant differences between the two species (Figure S7), indicating similar uptake rates of recently photosynthesized C by soil microorganisms.

Despite changes in C allocation below-ground depending on drought and species identity, the active rhizosphere microbial community utilizing N and C was not affected by species identity or drought treatment (Figure S8). However, we found evidence for small, but consistent changes in the pattern of ^{13}C allocation to different fatty acid biomarkers caused by drought and species (Figure 4), as well as a few changes in specific bacterial families (Figure S10; Table S6), such as Enterobacteriaceae and Rhizobiaceae. Although not all the pairwise comparison were significantly different and these results should be interpreted with caution, the first family includes taxa that are common drought-tolerant plant growth-promoting rhizobacteria (Ahmed et al., 2021; Arora & Jha, 2023; Naveed et al., 2014). The second is a common N-fixing bacteria including both symbiotic nitrogen-fixers and free-living taxa, and can promote growth and drought tolerance (Barquero et al., 2022; Fahde et al., 2023). Furthermore, the nutrient acquisition strategies of the soil microbial community under subordinate species shifted to higher investments into acquisition of C-rich compounds, both in drought and control conditions (Figure 5). Recent studies have shown that soil microbial communities subjected to long-term drought shift allocation towards C-obtaining enzymes, over N and P (Asensio et al., 2021; Canarini et al., 2021). Thus, overall, our results indicate that subordinate species may foster processes typical of microbial communities previously exposed to drought. While our pulse-labelling approach only represents a snapshot of time dynamics, we reveal small but consistent patterns in rhizodeposition and knock-on effects on the microbial community and its resource acquisition strategies that might determine larger ecosystem responses when integrated over longer time scales. Importantly, these strategies were consistent across the two field experiments, despite the differences in soil properties and soil microbial communities.

The dominant plant species not only had lower accumulation of rhizodeposits below-ground, but also displayed higher C:N ratio in above-ground biomass and lower soil N uptake rates, when compared to the subordinate species. Hence, our results indicate two different strategies between dominant and subordinate species. The dominant species invests more C above-ground per unit of N, a feature that might favour dominance when soil moisture and nutrients are available. The subordinate species, on the other hand, invests more C below-ground and obtains more N than the dominant species during drought,

a feature that might allow greater resistance during drought periods when nutrient mobility in soil becomes limited. This supports previous experiments showing that removal of subordinate species causes a loss of ecosystem functioning (i.e. soil respiration) during drought (Mariotte et al., 2015). We speculate that these two different strategies contribute to plant community dynamics during drought (i.e. greater biomass loss of dominant species favouring subordinate species) observed in field experiments (Mariotte, 2014; Mariotte et al., 2017; Mariotte, Vandenberghe, Kardol, et al., 2013). However, our experiment only analysed two individual species and in order to generalize these findings more research is needed. In addition, our results reveal that, under drought stress, the subordinate species *C. dactylon* was able to strengthen its association with arbuscular mycorrhizal fungi, as evidenced by higher colonization rates and arbuscule formation compared to the dominant species (Figure 3), which support previous findings (Mariotte et al., 2017). Interestingly, the level of C supply to arbuscular mycorrhizal fungi was not different between the two species. Thus, our results indicate that subordinate species can acquire more N with the same investment of C to mycorrhizae, compared to the dominant species, possibly suggesting a lower C to N cost. Evidence that the nutrient cost-to-benefit ratio in arbuscular mycorrhizal associations varies among different host plant species is accumulating (Wipf et al., 2019). These differences are found even within varieties of the same species, as shown for wheat (Thirkell et al., 2020). However, while NanoSIMS images show that the mycorrhizal pathway was used to deliver N and obtain C (Figure S5) within roots (image obtained only for the dominant plant species), our results cannot quantitatively differentiate between N uptake pathways (direct or mycorrhizal), and further evidence is necessary to support these conclusions. The absence of NanoSIMS data for *C. dactylon*, also restrict our ability to confirm AMF-mediated nutrient dynamics across species.

Lastly, under control conditions, the subordinate species exhibited high values of photosynthesized C and N uptake, and C transfer to the microbial community, similar to the dominant species. The fact that subordinate species performed similarly to the dominant species was surprising, given the difference in dominance that these two species attain within natural communities. However, a recent experiment has shown that when grown in isolation these two species can perform similarly in well-watered conditions, whereas *P. dilatatum* shoot and root biomass were more strongly affected by drought (Barnett et al., 2018). Furthermore, subordinate species have shown increased competitive ability when root competition is removed (Mariotte et al., 2012). Our experiment, by isolating the two species, allowed us to study species-specific interactions with the soil biota, but simultaneously released competition dynamics between dominant and subordinate species. In field conditions, dominant species might quickly build up a higher amount of biomass by investing more C per unit of N and increase their competitive ability (in terms of light). Therefore, our subordinate control treatment likely experienced conditions that do not resemble natural scenarios (Mariotte et al., 2017).

In conclusion, we found that the subordinate species increased C allocation below-ground and N uptake in response to drought, compared to the dominant species. This translated into small but consistent effects on the active soil microbial community, as well as changes in the allocation of enzyme for soil C acquisition relative to nutrients. Therefore, our results suggest that the subordinate species achieves higher drought resistance in biomass and soil functions via increased below-ground activity. Research on relating relative species abundance to functional traits is still lacking, reducing our ability to predict larger ecosystem responses to climate change, such as community change and soil C emissions. While our study only included two species, the data presented here provide a basis to explain the underlying mechanisms behind the response of grassland communities and their C cycling to drought.

AUTHOR CONTRIBUTIONS

Pierre Mariotte, Barbara Drigo and Yolima Carrillo designed the original experimental plan with contributions from Sally A. Power, Erica Donner and Ian C. Anderson. Alberto Canarini and Feike A. Dijkstra designed the JP field site experiment, while Sally A. Power and Raúl Ochoa-Hueso designed the DG field experiment. Alberto Canarini, Pierre Mariotte, Barbara Drigo, Yolima Carrillo and Raúl Ochoa-Hueso carried out the field harvest and the laboratory analyses. NanoSIMS images were generated and analysed by Jeremy Bougoure. Amplicon sequencing data were processed by Sotirios Vasileiadis and further analysed by Barbara Drigo, Alberto Canarini and Hirokazu Toju. Remaining data were analysed by Alberto Canarini with the contribution of Pierre Mariotte, Andreas Richter, Barbara Drigo, Raúl Ochoa-Hueso and Yolima Carrillo. Alberto Canarini, Pierre Mariotte, Raúl Ochoa-Hueso, Yolima Carrillo and Barbara Drigo wrote the original draft. All authors contributed critically to the drafts and gave final approval for publication.

ACKNOWLEDGEMENTS

This project was supported by the University of South Australia (Research Themes Investment Scheme (RTIS): PG103515), the South Australian Government (SA PRIF IRGP 45), the Australian Research Council (n. FT130101003 and n. FT100100779) and by the Hawkesbury Institute for the Environment, Soil Biology and Genomics Theme Seed Grant. A.C. received financial support as an International Research Fellow of Japan Society for the Promotion of Science [Postdoctoral Fellowships for Research in Japan (Standard)]. This work was supported by the European Research Council (ERC) under the EU's Horizon Europe programme (grant agreement No 101115960, EcoMEMO). Views and opinions expressed are, however, those of the author(s) only and do not necessarily reflect those of the European Union or the European Research Council Executive Agency. Neither the European Union nor the granting authority can be held responsible for them. The authors declare that the funding bodies had no direct influence on the study design, collection, analysis/interpretation of data or in the writing of this report. We are grateful to all who aided in facilitating this research, e.g. assisting with site access, providing advice and discussing results. Open access publishing facilitated by Adelaide University, as part of the Wiley - Adelaide University agreement via the Council of Australasian University Librarians.

CONFLICT OF INTEREST STATEMENT

Authors declare that they have no competing interests. Pierre Mariotte is a Senior Editor of Journal of Ecology, but took no part in the peer review and decision-making processes for this paper.

PEER REVIEW

The peer review history for this article is available at https://www.webofscience.com/api/gateway/wos/peer-review/10.1111/1365-2745.70289.

DATA AVAILABILITY STATEMENT

The data that support the main findings of this study will be openly available upon publication in the GitHub repository at https://github.com/acanarini/Subordinate_Drought with the following: https://doi.org/10.5281/zenodo.18705754 (Canarini et al., 2026). The sequencing data are available in the NCBI Sequence Read Archive under BioProject accession number PRJNA1143436.

ORCID

Alberto Canarini https://orcid.org/0000-0003-2516-5955
Pierre Mariotte https://orcid.org/0000-0001-8570-8742
Yolima Carrillo https://orcid.org/0000-0002-8726-4601
Raúl Ochoa-Hueso https://orcid.org/0000-0002-1839-6926
Jeremy Bougoure https://orcid.org/0000-0002-4869-035X
Sotirios Vasileiadis https://orcid.org/0000-0002-2048-8192
Ian C. Anderson https://orcid.org/0000-0002-3507-163X
Feike A. Dijkstra https://orcid.org/0000-0002-6191-6018
Andreas Richter https://orcid.org/0000-0003-3282-4808
Hirokazu Toju https://orcid.org/0000-0002-3362-3285
Erica Donner https://orcid.org/0000-0001-6465-2233
Sally A. Power https://orcid.org/0000-0002-2723-8671
Barbara Drigo https://orcid.org/0000-0002-3301-0470

REFERENCES

Ahmed, B., Shahid, M., Syed, A., Rajput, V. D., Elgorban, A. M., Minkina, T., Bahkali, A. H., & Lee, J. (2021). Drought tolerant *Enterobacter* sp./*Leclercia adecarboxylata* secretes Indole-3-acetic acid and other biomolecules and enhances the biological attributes of *Vigna radiata* (L.) R. Wilczek in water deficit conditions. *Biology*, *10*, 1149.

Arora, S., & Jha, P. N. (2023). Drought-tolerant *Enterobacter bugandensis* WRS7 induces systemic tolerance in *Triticum aestivum* L. (wheat) under drought conditions. *Journal of Plant Growth Regulation*, *42*, 7715–7730.

Asensio, D., Zuccarini, P., Ogaya, R., Marañón-Jiménez, S., Sardans, J., & Peñuelas, J. (2021). Simulated climate change and seasonal drought increase carbon and phosphorus demand in Mediterranean forest soils. *Soil Biology and Biochemistry*, *163*, 108424.

Banerjee, S., Schlaeppi, K., & van der Heijden, M. G. A. (2018). Keystone taxa as drivers of microbiome structure and functioning. *Nature Reviews Microbiology*, *16*, 567–576.

Barnett, K. L., Johnson, S. N., & Power, S. A. (2018). Drought negates growth stimulation due to root herbivory in pasture grasses. *Oecologia*, *188*, 777–789.

Barquero, M., Poveda, J., Laureano-Marín, A. M., Ortiz-Liébana, N., Brañas, J., & González-Andrés, F. (2022). Mechanisms involved in drought stress tolerance triggered by rhizobia strains in wheat. *Frontiers in Plant Science*, *13*, 1036973.

Bell, C. W., Fricks, B. E., Rocca, J. D., Steinweg, J. M., McMahon, S. K., & Wallenstein, M. D. (2013). High-throughput fluorometric measurement of potential soil extracellular enzyme activities. *Journal of Visualized Experiments*, *81*, e50961.

Berry, D., Ben Mahfoudh, K., Wagner, M., & Loy, A. (2011). Barcoded primers used in multiplex amplicon pyrosequencing bias amplification. *Applied and Environmental Microbiology*, *77*, 7846–7849.

Bever, J. D., Dickie, I. A., Facelli, E., Facelli, J. M., Klironomos, J., Moora, M., Rillig, M. C., Stock, W. D., Tibbett, M., & Zobel, M. (2010). Rooting theories of plant community ecology in microbial interactions. *Trends in Ecology & Evolution*, *25*, 468–478.

Bligh, E. G., & Dyer, W. J. (1959). A rapid method of total lipid extraction and purification. *Canadian Journal of Biochemistry and Physiology*, *37*, 911–917.

Boeken, B., & Shachak, M. (2006). Linking community and ecosystem processes: The role of minor species. *Ecosystems*, *9*, 119–127.

Bougoure, J., Ludwig, M., Brundrett, M., Cliff, J., Clode, P., Kilburn, M., & Grierson, P. (2014). High-resolution secondary ion mass spectrometry analysis of carbon dynamics in mycorrhizas formed by an obligately myco-heterotrophic orchid. *Plant, Cell & Environment*, *37*, 1223–1230.

Buyer, J. S., & Sasser, M. (2012). High throughput phospholipid fatty acid analysis of soils. *Applied Soil Ecology*, *61*, 127–130.

Canarini, A., Carrillo, Y., Mariotte, P., Ingram, L., & Dijkstra, F. A. (2016). Soil microbial community resistance to drought and links to C stabilization in an Australian grassland. *Soil Biology and Biochemistry*, *103*, 171–180.

Canarini, A., Kaiser, C., Merchant, A., Richter, A., & Wanek, W. (2019). Root exudation of primary metabolites: Mechanisms and their roles in plant responses to environmental stimuli. *Frontiers in Plant Science*, *10*, 422679.

Canarini, A., Mariotte, P., Carrillo, Y., Ochoa-Hueso, R., Bougoure, J., Vasileiadis, S., Anderson, I. C., Dijkstra, F. A., Richter, A., Toju, H., Donner, E., Power, S. A., & Drigo, B. (2026). Data from: Enhanced belowground functioning is associated with higher plant resistance against drought: Implications for ecosystem functions [data set]. *Zenodo*. https://doi.org/10.5281/zenodo.18705754

Canarini, A., Merchant, A., & Dijkstra, F. A. (2016). Drought effects on Helianthus annuus and Glycine max metabolites: From phloem to root exudates. *Rhizosphere*, *2*, 85–97.

Canarini, A., Schmidt, H., Fuchslueger, L., Martin, V., Herbold, C. W., Zezula, D., Gündler, P., Hasibeder, R., Jecmenica, M., Bahn, M., & Richter, A. (2021). Ecological memory of recurrent drought modifies soil processes via changes in soil microbial community. *Nature Communications*, *12*, 5308.

Castañeda-Gómez, L., Walker, J. K. M., Powell, J. R., Ellsworth, D. S., Pendall, E., & Carrillo, Y. (2020). Impacts of elevated carbon dioxide on carbon gains and losses from soil and associated microbes in a Eucalyptus woodland. *Soil Biology and Biochemistry*, *143*, 107734.

Castillioni, K., Wilcox, K., Jiang, L., Luo, Y., Jung, C. G., & Souza, L. (2020). Drought mildly reduces plant dominance in a temperate prairie ecosystem across years. *Ecology and Evolution*, *10*, 6702–6713.

Conant, R. T., Ryan, M. G., Ågren, G. I., Birge, H. E., Davidson, E. A., Eliasson, P. E., Evans, S. E., Frey, S. D., Giardina, C. P., Hopkins, F. M., Hyvönen, R., Kirschbaum, M. U. F., Lavallee, J. M., Leifeld, J., Parton, W. J., Megan Steinweg, J., Wallenstein, M. D., Martin Wetterstedt, J. Å., & Bradford, M. A. (2011). Temperature and soil organic matter decomposition rates—Synthesis of current knowledge and a way forward. *Global Change Biology*, *17*, 3392–3404.

de Vries, F. T., Manning, P., Tallowin, J. R. B., Mortimer, S. R., Pilgrim, E. S., Harrison, K. A., Hobbs, P. J., Quirk, H., Shipley, B., Cornelissen, J. H. C., Kattge, J., & Bardgett, R. D. (2012). Abiotic drivers and plant traits explain landscape-scale patterns in soil microbial communities. *Ecology Letters*, *15*, 1230–1239.

de Vries, F. T., Williams, A., Stringer, F., Willcocks, R., McEwing, R., Langridge, H., & Straathof, A. L. (2019). Changes in

root-exudate-induced respiration reveal a novel mechanism through which drought affects ecosystem carbon cycling. *New Phytologist*, *224*, 132–145.

Diaz, S., Hodgson, J. G., Thompson, K., Cabido, M., Cornelissen, J. H. C., Jalili, A., Montserrat-Martí, G., Grime, J. P., Zarrinkamar, F., Asri, Y., Band, S. R., Basconcelo, S., Castro-Díez, P., Funes, G., Hamzehee, B., Khoshnevi, M., Pérez-Harguindeguy, N., Pérez-Rontomé, M. C., Shirvany, F. A., … Zak, M. R. (2004). The plant traits that drive ecosystems: Evidence from three continents. *Journal of Vegetation Science*, *15*, 295–304.

Drigo, B., Pijl, A. S., Duyts, H., Kielak, A. M., Gamper, H. A., Houtekamer, M. J., Boschker, H. T. S., Bodelier, P. L. E., Whiteley, A. S., van Veen, J. A., & Kowalchuk, G. A. (2010). Shifting carbon flow from roots into associated microbial communities in response to elevated atmospheric CO_2. *Proceedings of the National Academy of Sciences of the United States of America*, *107*, 10938–10942.

Fahde, S., Boughribil, S., Sijilmassi, B., & Amri, A. (2023). Rhizobia: A promising source of plant growth-promoting molecules and their non-legume interactions: Examining applications and mechanisms. *Agriculture*, *13*, 1279.

Frank, D. N. (2009). BARCRAWL and BARTAB: Software tools for the design and implementation of barcoded primers for highly multiplexed DNA sequencing. *BMC Bioinformatics*, *10*, 362.

Frostegård, Å., Tunlid, A., & Bååth, E. (2011). Use and misuse of PLFA measurements in soils. *Soil Biology and Biochemistry*, *43*, 1621–1625.

Grigulis, K., Lavorel, S., Krainer, U., Legay, N., Baxendale, C., Dumont, M., Kastl, E., Arnoldi, C., Bardgett, R. D., Poly, F., Pommier, T., Schloter, M., Tappeiner, U., Bahn, M., & Clément, J. C. (2013). Relative contributions of plant traits and soil microbial properties to mountain grassland ecosystem services. *Journal of Ecology*, *101*, 47–57.

Grime, J. P. (1998). Benefits of plant diversity to ecosystems: Immediate, filter and founder effects. *Journal of Ecology*, *86*, 902–910.

Grime, J. P., Thompson, K., Hunt, R., Hodgson, J. G., Cornelissen, J. H. C., Rorison, I. H., Hendry, G. A. F., Ashenden, T. W., Askew, A. P., Band, S. R., Booth, R. E., Bossard, C. C., Campbell, B. D., Cooper, J. E. L., Davison, A. W., Gupta, P. L., Hall, W., Hand, D. W., Hannah, M. A., … Whitehouse, J. (1997). Integrated screening validates primary axes of specialisation in plants. *Oikos*, *79*, 259–281.

Hu, Y., Zheng, Q., Zhang, S., Noll, L., & Wanek, W. (2018). Significant release and microbial utilization of amino sugars and d-amino acid enantiomers from microbial cell wall decomposition in soils. *Soil Biology and Biochemistry*, *123*, 115–125.

Hursh, A., Ballantyne, A., Cooper, L., Maneta, M., Kimball, J., & Watts, J. (2017). The sensitivity of soil respiration to soil temperature, moisture, and carbon supply at the global scale. *Global Change Biology*, *23*, 2090–2103.

IPCC. (2023). *Climate change 2023: Synthesis report. Contribution of working groups I, II and III to the sixth assessment report of the intergovernmental panel on climate change* (Core Writing Team, H. Lee, & J. Romero).

Jia, Y., Walder, F., Wagg, C., & Feng, G. (2021). Mycorrhizal fungi maintain plant community stability by mitigating the negative effects of nitrogen deposition on subordinate species in Central Asia. *Journal of Vegetation Science*, *32*, e12944.

Karlowsky, S., Augusti, A., Ingrisch, J., Akanda, M. K. U., Bahn, M., & Gleixner, G. (2018). Drought-induced accumulation of root exudates supports post-drought recovery of microbes in mountain grassland. *Frontiers in Plant Science*, *9*, 1593.

Kozak, M., & Piepho, H. (2018). What's normal anyway? Residual plots are more telling than significance tests when checking ANOVA assumptions. *Journal of Agronomy and Crop Science*, *204*, 86–98.

Lavorel, S., Grigulis, K., Lamarque, P., Colace, M.-P., Garden, D., Girel, J., Pellet, G., & Douzet, R. (2011). Using plant functional traits to understand the landscape distribution of multiple ecosystem services. *Journal of Ecology*, *99*, 135–147.

Lin, G., McCormack, M. L., & Guo, D. (2015). Arbuscular mycorrhizal fungal effects on plant competition and community structure. *Journal of Ecology*, *103*, 1224–1232.

Lin, H., & Peddada, S. D. (2024). Multigroup analysis of compositions of microbiomes with covariate adjustments and repeated measures. *Nature Methods*, *21*, 83–91.

Mariotte, P. (2014). Do subordinate species punch above their weight? Evidence from above- and below-ground. *New Phytologist*, *203*, 16–21.

Mariotte, P., Buttler, A., Johnson, D., Thébault, A., & Vandenberghe, C. (2012). Exclusion of root competition increases competitive abilities of subordinate plant species through root–shoot interactions. *Journal of Vegetation Science*, *23*, 1148–1158.

Mariotte, P., Canarini, A., & Dijkstra, F. A. (2017). Stoichiometric N:P flexibility and mycorrhizal symbiosis favour plant resistance against drought. *Journal of Ecology*, *105*, 958–967.

Mariotte, P., Meugnier, C., Johnson, D., Thébault, A., Spiegelberger, T., & Buttler, A. (2013). Arbuscular mycorrhizal fungi reduce the differences in competitiveness between dominant and subordinate plant species. *Mycorrhiza*, *23*, 267–277.

Mariotte, P., Robroek, B. J. M., Jassey, V. E. J., & Buttler, A. (2015). Subordinate plants mitigate drought effects on soil ecosystem processes by stimulating fungi. *Functional Ecology*, *29*, 1578–1586.

Mariotte, P., Vandenberghe, C., Kardol, P., Hagedorn, F., & Buttler, A. (2013). Subordinate plant species enhance community resistance against drought in semi-natural grasslands. *Journal of Ecology*, *101*, 763–773.

Mariotte, P., Vandenberghe, C., Meugnier, C., Rossi, P., Bardgett, R. D., & Buttler, A. (2013). Subordinate plant species impact on soil microbial communities and ecosystem functioning in grasslands: Findings from a removal experiment. *Perspectives in Plant Ecology, Evolution and Systematics*, *15*, 77–85.

McGonigle, T. P., Miller, M. H., Evans, D. G., Fairchild, G. L., & Swan, J. A. (1990). A new method which gives an objective measure of colonization of roots by vesicular—Arbuscular mycorrhizal fungi. *New Phytologist*, *115*, 495–501.

McMurdie, P. J., & Holmes, S. (2013). Phyloseq: An R package for reproducible interactive analysis and graphics of microbiome census Data. *PLoS One*, *8*, e61217.

Mojzes, A., Ónodi, G., Lhotsky, B., Kalapos, T., Csontos, P., & Kröel-Dulay, G. (2018). Within-generation and transgenerational plasticity in growth and regeneration of a subordinate annual grass in a rainfall experiment. *Oecologia*, *188*, 1059–1068.

Naveed, M., Mitter, B., Reichenauer, T. G., Wieczorek, K., & Sessitsch, A. (2014). Increased drought stress resilience of maize through endophytic colonization by *Burkholderia phytofirmans* PsJN and *Enterobacter* sp. FD17. *Environmental and Experimental Botany*, *97*, 30–39.

Ochoa-Hueso, R., Arca, V., Delgado-Baquerizo, M., Hamonts, K., Piñeiro, J., Serrano-Grijalva, L., Shawyer, J., & Power, S. A. (2020). Links between soil microbial communities, functioning, and plant nutrition under altered rainfall in Australian grassland. *Ecological Monographs*, *90*, e01424.

Oksanen, J., Blanchet, F. G., Kindt, R., Legendre, P., Minchin, P. R., O'hara, R. B., Simpson, G. L., Solymos, P., Stevens, M. H., & Wagner, H. (2013). Vegan: Community ecology package version 2.0-10. *Journal of Statistical Software*, *48*(9), 103–132.

Olsson, P. A., & Lekberg, Y. (2022). A critical review of the use of lipid signature molecules for the quantification of arbuscular mycorrhiza fungi. *Soil Biology and Biochemistry*, *166*, 108574.

Petermann, J. S., & Buzhdygan, O. Y. (2021). Grassland biodiversity. *Current Biology*, *31*, R1195–R1201.

Pinheiro, J., Bates, D., DebRoy, S., Sarkar, D., & R Core Team. (2017). nlme: Linear and nonlinear mixed effects models. Version 3. https://CRAN.R-project.org/package=nlme

Power, S. A., Barnett, K. L., Ochoa-Hueso, R., Facey, S. L., Gibson-Forty, E. V. J., Hartley, S. E., Nielsen, U. N., Tissue, D. T., & Johnson, S. N. (2016). DRI-grass: A new experimental platform for addressing grassland ecosystem responses to future precipitation scenarios in south-East Australia. *Frontiers in Plant Science*, *7*, 1373.

Pugnaire, F. I., Morillo, J. A., Peñuelas, J., Reich, P. B., Bardgett, R. D., Gaxiola, A., Wardle, D. A., & van der Putten, W. H. (2019). Climate change effects on plant-soil feedbacks and consequences for biodiversity and functioning of terrestrial ecosystems. *Science Advances*, *5*, eaaz1834.

Qin, S., Chen, L., Fang, K., Zhang, Q., Wang, J., Liu, F., Yu, J., & Yang, Y. (2019). Temperature sensitivity of SOM decomposition governed by aggregate protection and microbial communities. *Science Advances*, *5*, eaau1218.

R Core Team. (2020). *R: A language and environment for statistical computing*. R Foundation for Statistical Computing.

Roesch, L. F. W., Dobbler, P. T., Pylro, V. S., Kolaczkowski, B., Drew, J. C., & Triplett, E. W. (2020). Pime: A package for discovery of novel differences among microbial communities. *Molecular Ecology Resources*, *20*, 415–428.

Sharma, M. P., & Buyer, J. S. (2015). Comparison of biochemical and microscopic methods for quantification of arbuscular mycorrhizal fungi in soil and roots. *Applied Soil Ecology*, *95*, 86–89.

Sinsabaugh, R. L., Lauber, C. L., Weintraub, M. N., Ahmed, B., Allison, S. D., Crenshaw, C., Contosta, A. R., Cusack, D., Frey, S., Gallo, M. E., Gartner, T. B., Hobbie, S. E., Holland, K., Keeler, B. L., Powers, J. S., Stursova, M., Takacs-Vesbach, C., Waldrop, M. P., Wallenstein, M. D., … Zeglin, L. H. (2008). Stoichiometry of soil enzyme activity at global scale. *Ecology Letters*, *11*, 1252–1264.

Straub, D., Blackwell, N., Langarica-Fuentes, A., Peltzer, A., Nahnsen, S., & Kleindienst, S. (2020). Interpretations of environmental microbial community studies are biased by the selected 16S rRNA (gene) amplicon sequencing pipeline. *Frontiers in Microbiology*, *11*, 2652.

Thirkell, T. J., Pastok, D., & Field, K. J. (2020). Carbon for nutrient exchange between arbuscular mycorrhizal fungi and wheat varies according to cultivar and changes in atmospheric carbon dioxide concentration. *Global Change Biology*, *26*, 1725–1738.

Urcelay, C., & Díaz, S. (2003). The mycorrhizal dependence of subordinates determines the effect of arbuscular mycorrhizal fungi on plant diversity. *Ecology Letters*, *6*, 388–391.

Van Der Heijden, M. G. A., Bardgett, R. D., & Van Straalen, N. M. (2008). The unseen majority: Soil microbes as drivers of plant diversity and productivity in terrestrial ecosystems. *Ecology Letters*, *11*, 296–310.

Van Dyke, M. N., Levine, J. M., & Kraft, N. J. B. (2022). Small rainfall changes drive substantial changes in plant coexistence. *Nature*, *611*, 507–511.

Vierheilig, H., Coughlan, A. P., Wyss, U., & Piche, Y. (1998). Ink and vinegar, a simple staining technique for arbuscular-mycorrhizal fungi. *Applied and Environmental Microbiology*, *64*, 5004–5007.

Wagg, C., Bender, S. F., Widmer, F., & van der Heijden, M. G. A. (2014). Soil biodiversity and soil community composition determine ecosystem multifunctionality. *Proceedings of the National Academy of Sciences of the United States of America*, *111*, 5266–5270.

Waring, B. G., Weintraub, S. R., & Sinsabaugh, R. L. (2014). Ecoenzymatic stoichiometry of microbial nutrient acquisition in tropical soils. *Biogeochemistry*, *117*, 101–113.

Wickham, H. (2016). *ggplot2-elegant graphics for Data analysis*. Springer International Publishing.

Williams, A., & de Vries, F. T. (2020). Plant root exudation under drought: Implications for ecosystem functioning. *New Phytologist*, *225*, 1899–1905.

Williams, A., Langridge, H., Straathof, A. L., Muhamadali, H., Hollywood, K. A., Goodacre, R., & de Vries, F. T. (2021). Root functional traits explain root exudation rate and composition across a range of grassland species. *Journal of Ecology*, *110*, 21–33.

Wipf, D., Krajinski, F., van Tuinen, D., Recorbet, G., & Courty, P.-E. (2019). Trading on the arbuscular mycorrhiza market: From arbuscules to common mycorrhizal networks. *New Phytologist*, *223*, 1127–1142.

Yao, Q., Zhu, H.-H., Hu, Y.-L., & Li, L.-Q. (2008). Differential influence of native and introduced arbuscular mycorrhizal fungi on growth of dominant and subordinate plants. *Plant Ecology*, *196*, 261–268.

Yu, Q., Wilcox, K., La Pierre, K., Knapp, A. K., Han, X., & Smith, M. D. (2015). Stoichiometric homeostasis predicts plant species dominance, temporal stability, and responses to global change. *Ecology*, *96*, 2328–2335.

SUPPORTING INFORMATION

Additional supporting information can be found online in the Supporting Information section at the end of this article.

Figure S1. Mean above-ground biomass ($g\,m^{-2}$) of dominant and subordinate species in control and drought plots at the DG and JP sites calculated from biomass sorting at the species-group level in 2015.

Figure S2. Rarefaction curves obtained for the 16S rRNA and ITS datasets.

Figure S3. Graph showing effects of drought, species and sites on (a) below-ground and (b) above-ground biomass (mg pot^{-1}), (c) root: shoot biomass ratio and (d) shoot C:N ratio.

Figure S4. Graph showing effects of drought, species and sites on (a) bulk soil ^{13}C (mg $^{13}C\,g^{-1}$ dm) and (b) root: shoot ratio of ^{13}C amounts excess.

Figure S5. Paspalum dilatatum (dominant; non-drought) root cross section from plant labelled with $^{13}CO_2$ and $^{15}N\text{-}NH_4/NO_3$ showing an obvious fungal arbuscule structure within a single root cortical cell.

Figure S6. Graph showing effects of drought, species and sites on (a) mycorrhizal root colonization (%); (b) arbuscular mycorrhiza PLFA biomarker (nmol C g $soil^{-1}$); (c) ^{13}C in the arbuscular mycorrhiza NLFA biomarker (nmol ^{13}C g $soil^{-1}$) and (d) ^{13}C in the arbuscular mycorrhiza PLFA biomarker (nmol ^{13}C g $soil^{-1}$).

Figure S7. Graph showing effects of drought, species and sites on taxonomic groups, grouped using PLFA biomarker.

Figure S8. Graphs showing effects of drought, species and sites from the RNA-SIP dataset.

Figure S9. Graph showing effects of drought, species and sites on gene copy numbers obtained by qPCR for: (a) 16S dataset and (b) ITS dataset.

Figure S10. Graph showing effects of drought, species and sites on read counts normalized by gene copy numbers of the 16S (g^{-1} dry soil) from qPCR (Figure S7).

Table S1. Climate, soil properties (top 10 cm) and list of the dominant and subordinate species of the two sites.

Table S2. Statistical analysis results of plant and soil variables.

Table S3. Statistical analyses on arbuscular mycorrhizal data. Hyphal and arbuscules colonization rates are expressed in % (as explained in Section 2).

BRITISH ECOLOGICAL SOCIETY Journal of Ecology

Table S4. Statistical analyses of other microbial groups (PLFA).

Table S5. Multivariate statistical analyses (PERMANOVA) performed with the function *adonis* of the R package 'vegan', as described in Section 2.

Table S6. ANCOM-BC2 results from the pairwise and global analysis (last column) on the data obtained via RNA-SIP analysis.

Table S7. Statistical analyses of the stoichiometric ratio of enzyme activities.

How to cite this article: Canarini, A., Mariotte, P., Carrillo, Y., Ochoa-Hueso, R., Bougoure, J., Vasileiadis, S., Anderson, I. C., Dijkstra, F. A., Richter, A., Toju, H., Donner, E., Power, S. A., & Drigo, B. (2026). Enhanced below-ground functioning is associated with higher plant resistance against drought: Implications for ecosystem functions. *Journal of Ecology*, *114*, e70289. https://doi.org/10.1111/1365-2745.70289